Int. J. Nonlinear Anal. Appl. 13 (2022) 2, 2059–2070
ISSN: 2008-6822 (electronic)
http://dx.doi.org/10.22075/ijnaa.2022.6753

Numerical investigation of the solitary and periodic waves in the nonlocal discrete Manakov system

Ahmed Fawaz Al-Saffawi*, Sohaib Talal Al-Ramadhani

Department of Mathematics, College of Education for Pure Sciences, University of Mosul, Mosul, Iraq

(Communicated by Javad Vahidi)

Abstract

Solitary waves are interesting phenomena arising in various fields of physics, chemistry, and biology. Nonlinear continuous and discrete models supporting wave solutions of solitary behaviour have received increasing attention in recent years. Some examples of such integrable systems include Korteweg de-Vries (KdV) equation, the nonlinear Schrödinger (NLS) equation, and the Manakov system (MS). In this paper, we propose a discrete nonlocal version of the nonlinear Manakov system which admits spatial and temporal PT-symmetry. PT-symmetry property gives relevance to various fields in physics and has received a lot of attention in the studies of integrable nonlinear equations. In this work, the time evolution of solitary and periodic wave solutions in the proposed system has been numerically investigated. Suitable initial conditions have been considered to construct bright and dark solitons. The variational iteration method (VIM) was used to simulate the solution of the system. The error measurement of the simulation demonstrates the efficiency of the numerical method in constructing the different types of wave solutions.

Keywords: integrable systems, PT-symmetry, solitons, nonlocal discrete Manakov system, approximate solution, variational iteration method
2020 MSC: 35C08

1 Introduction

Integrable nonlinear evolutionary equations play an important role in the field of mathematical physics, including nonlinear wave propagation, plasma physics, Bose-Einstein condensates, nonlinear optics and ocean waves [56]. In addition to the property of complete solvability, integrable systems exhibit another interesting mathematical feature of having an infinite number of constants of motion according to the validity of an infinite number of conservation laws [5]. A special class of solutions that might arise from such an integrable system is the solitary wave also called a soliton. Solitons have been observed experimentally in many fields such as physics, chemistry and biology. The solitary wave phenomena might be attributed to a special balance between wave steepening and other physical effects such as dispersion and diffraction [5].

Integrable mathematical models are often local equations, which means that the development of the solution depends only on the value of the local solution and its local spatial and temporal derivatives, for example, the Korteweg de-Vries (KdV) equation, the Sine-Gordon (SG) equation, and the nonlinear Schrödinger (NLS) equation

*Corresponding author
Email addresses: ahmed.20esp1@student.uomosul.edu.iq (Ahmed Fawaz Al-Saffawi), s.alramadhani@uomosul.edu.iq (Sohaib Talal Al-Ramadhani)

Received: February 2022 *Accepted:* June 2022

[28, 55]. However, many nonlocal integrable models have also been proposed and the investigation of the dynamics of such nonlocal systems is an active topic of research [56].

A special class of local and nonlocal systems is when the dynamics of the solution are symmetric in time and space, which is referred to as parity-time (PT)-symmetric. Integrable systems satisfying the PT-symmetry have both physical and mathematical perspectives and have attracted considerable attention in recent years (see [9, 11, 15, 18, 22, 26, 27, 32, 37, 41, 42, 43, 48]).

An interesting example of integrable nonlocal systems is the nonlocal nonlinear Schrödinger (NNLS) equation proposed by Ablowitz and Musslimani in the form [3]:

$$i\mathcal{Q}_t(x,t)+\mathcal{Q}_{xx}(x,t)+2\sigma\mathcal{Q}^2(x,t)\,\mathcal{Q}^*(-x,t)=0,\quad i=\sqrt{(-1)},\quad \sigma=\pm1 \tag{1.1}$$

where $\mathcal{Q}(x,t)$ is a complex-valued function of the two real variables x and t, the symbol $*$ represents complex conjugation. The case when $(\sigma=1)$ in equation (1.1) is called as focusing case, while the case $(\sigma=-1)$ is referred to as the defocusing case. The solution states at distant locations x and $-x$ are directly coupled in this equation. The nonlinear term in the NNLS equation represents a self-induced potential that can be written in the form $\mathcal{W}(x,t)=\mathcal{Q}(x,t)\,\mathcal{Q}^*(-x,t)$, which satisfies the PT-symmetry condition $\mathcal{W}(x,t)=\mathcal{W}^*(-x,t)$. This means that equation (1.1) remains invariant under the replacements $x\to-x$ and $t\to-t$ after taking the complex conjugate [4]. This gives relevance to the field of PT-symmetric quantum mechanics, PT-symmetric optics, and other applications of PT-symmetric physics that are currently subject to much research activity [8, 14, 26].

A generalization of equation (1.1) is the two-component vector nonlocal nonlinear Schrödinger (VNNLS) equation, also called the nonlocal Manakov system (NMS) [24, 45, 46, 47], which has the formula:

$$\begin{array}{l} i\mathcal{Q}_t(x,t)+\mathcal{Q}_{xx}(x,t)+2\sigma\left[\mathcal{Q}(x,t)\,\mathcal{Q}^*(-x,t)+\mathcal{P}(x,t)\,\mathcal{P}^*(-x,t)\right]\mathcal{Q}(x,t)=0\\ i\mathcal{P}_t(x,t)+\mathcal{P}_{xx}(x,t)+2\sigma\left[\mathcal{Q}(x,t)\,\mathcal{Q}^*(-x,t)+\mathcal{P}(x,t)\,\mathcal{P}^*(-x,t)\right]\mathcal{P}(x,t)=0 \end{array},\ \sigma=\pm1 \tag{1.2}$$

where x is the spatial variable and t is the temporal variable and both are real. The two components $\mathcal{Q}(x,t)$, $\mathcal{P}(x,t)$ are two complex fields. The local Manakov system (MS) can be obtained by replacing the nonlocal fields $\mathcal{Q}^*(-x,t)$, $\mathcal{P}^*(-x,t)$ by $\mathcal{Q}^*(x,t)$, $\mathcal{P}^*(x,t)$, respectively [33]. The NMS possess self-induced potential $\mathcal{W}(x,t)=\mathcal{Q}(x,t)\,\mathcal{Q}^*(-x,t)+\mathcal{P}(x,t)\,\mathcal{P}^*(-x,t)$ and obeys the PT-symmetry condition. A number of studies have been published on the dynamics of solitons for the NMS [45, 49, 58, 59, 60]. In [45], the inverse scattering transform (IST) is used to provide a breathing one-soliton solution.

In 2014, Ablowitz and Musslimani [4] also suggested a discrete version of the NNLS equation (1.1) as a system of differential-difference equation given as:

$$i\mathcal{Q}_{n,t}+(\mathcal{Q}_{n+1}-2\mathcal{Q}_n+\mathcal{Q}_{n-1})+\sigma\mathcal{Q}_n\mathcal{Q}^*_{-n}(\mathcal{Q}_{n+1}+\mathcal{Q}_{n-1})=0,\quad \sigma=\pm1 \tag{1.3}$$

where $\mathcal{Q}_n$ is a complex function, here the index n is an integer representing the spatial variable on an infinite discrete space lattice, while t is the time variable. This system is integrable and hence, can be treated using the inverse scattering transform [4]. Sometimes equation (1.3) is also referred to as the integrable discrete nonlocal nonlinear Schrödinger (IDNNLS) equation [2, 4, 30]. Some of the important properties of the IDNNLS equation are contrasted with the integrable discrete nonlinear Schrödinger (IDNLS) equation in which the nonlocal nonlinear term $\mathcal{Q}_n\mathcal{Q}^*_{-n}$ is replaced by the local nonlinear term $|\mathcal{Q}_n|^2$ [4]. The IDNNLS equation is also a discrete PT-symmetric model [10], the nonlinear self-induced potential $\mathcal{W}_n=\mathcal{Q}_n\mathcal{Q}^*_{-n}$ guarantees that the equation is invariant under the combined symmetry of parity and time as shown in classical optics [35].

Following the generalization of the NNLS equation (1.1) to the NMS (1.2) in the continuous case, we can suggest a nonlocal discrete Manakov system (NDMS) as a coupled two-component IDNNLS equation of the form:

$$\begin{array}{l} i\mathcal{Q}_{n,t}+(\mathcal{Q}_{n+1}-2\mathcal{Q}_n+\mathcal{Q}_{n-1})+\sigma\left(\mathcal{Q}_n\mathcal{Q}^*_{-n}+\mathcal{P}_n\mathcal{P}^*_{-n}\right)(\mathcal{Q}_{n+1}+\mathcal{Q}_{n-1})=0\\ i\mathcal{P}_{n,t}+(\mathcal{P}_{n+1}-2\mathcal{P}_n+\mathcal{P}_{n-1})+\sigma(\mathcal{Q}_n\mathcal{Q}^*_{-n}+\mathcal{P}_n\mathcal{P}^*_{-n})(\mathcal{P}_{n+1}+\mathcal{P}_{n-1})=0 \end{array},\ \sigma=\pm1 \tag{1.4}$$

where $\mathcal{Q}_n$, $\mathcal{P}_n$ are two complex functions, n is an integer variable while t is a real variable. System (1.4) possess self-induced potential $\mathcal{W}_n(t)=\mathcal{Q}_n(t)\,\mathcal{Q}^*_{-n}(t)+\mathcal{P}_n(t)\mathcal{P}^*_{-n}(t)$ and it can be easily shown that $\mathcal{W}_n(t)=\mathcal{W}^*_{-n}(t)$. This means that the NDMS (1.4) remains invariant under the replacements $n\to-n$ and $t\to-t$ after taking the complex conjugate which obeys the PT-symmetry condition.

The solutions of the IDNNLS equation (1.3) has been explored in [4, 16, 21, 30, 31]. In this paper, we perform a numerical simulation for the solutions of the NDMS (1.4) using the variational iteration method (VIM).

The paper is organized as follows; in section two we briefly describe the VIM. In section three, suitable initial conditions are discussed to construct the solution of the NDMS via the iterative formula of the VIM. Section four is a description of the measurement tool for the numerical error of the approximation. A detailed description of the approximated solution for solitary and periodic wave solutions is presented in section five. The last section is a brief summary and conclusion of our study.

2 The Method of Variational Iteration

In 1999, Ji-Huan He introduced the variational iteration method (VIM) [19] to treat general nonlinear systems. Soon after, it has been widely utilized to solve ordinary and partial differential equations. The method has been verified to be efficient in solving both linear and nonlinear equations [12, 50, 51]. Here we introduce the VIM method's general idea; consider a general nonlinear system:

$$\mathcal{L}\,\mathcal{U}(t)+\mathcal{N}\,\mathcal{U}(t)=\mathcal{F}(t) \tag{2.1}$$

Here, $\mathcal{F}(t)$ is an analytic function, while $\mathcal{L}$ and $\mathcal{N}$ are linear and nonlinear operators, respectively. A correcting functional can be written as follows [6, 12, 29, 34, 36, 38, 39, 51, 57]:

$$\mathcal{U}_{k+1}(t)=\mathcal{U}_k(t)+\int_0^t \lambda(\tau)\ \left[\mathcal{L}\,\mathcal{U}_k(\tau)+\mathcal{N}\,\widetilde{\mathcal{U}}_k(\tau)-\mathcal{F}(\tau)\right]d\tau \tag{2.2}$$

where λ represents the Lagrange multiplier [38], which can be determined using variational theory. The index k indicates to the k^{th} iteration of the method, while $\widetilde{\mathcal{U}}_k$ specifies the constrained variation $\delta\widetilde{\mathcal{U}}_k=0$. Let λ be the optimal Lagrange multiplier and $\mathcal{U}_0$ be a function representing the initial condition, then the successive approximation $\mathcal{U}_{k+1}$ for $k\geq 0$ can be constructing according to the VIM as follows [34, 36]:

$$\mathcal{U}_{k+1}(t)=\mathcal{U}_k(t)+\int_0^t \lambda(\tau)\ \left[\mathcal{L}\,\mathcal{U}_k(\tau)+\mathcal{N}\,\mathcal{U}_k(\tau)-\mathcal{F}(\tau)\right]d\tau \tag{2.3}$$

3 Approximate Solutions

The behavior of the approximate solution is highly influenced by the selection of the initial condition. Here, a number of initial conditions are selected to construct the approximate solution of the NDMS (1.4) based on the analysis of similar integrable systems. The exact solutions of the NNLS equation are found in the references [5, 20, 21, 24, 31, 55]. The close form of a single soliton solution can be defined for the continuous NNLS equation (1.1) and if we consider the shape of the soliton's amplitude, then the soliton form can be generally described by the formula:

$$\mathcal{Q}(x,t)=\mathcal{A}e^{i(\alpha_1 x+\beta_1 t+\gamma_1)}\varphi(\alpha_2 x+\beta_2 t+\gamma_2) \tag{3.1}$$

where x and t are real variables, $\mathcal{A}$, α_j , β_j , γ_j ($j=1,2$) are real constants, $\mathcal{A}$ and φ describe, respectively, the highest absolute value and the shape of the wave amplitude after some normalization. The exponential part is related to the frequency and phase of the wave. Furthermore, the form of the single soliton solution for the continuous nonlocal Manakov system (CNMS) (1.2) was also given in [17, 24, 45], and as above can also be described as follows:

$$\begin{aligned}\mathcal{Q}(x,t)&=\mathcal{A}_1 e^{i(\alpha_1 x+\beta_1 t+\gamma_1)}\varphi(\alpha_2 x+\beta_2 t+\gamma_2)\\ \mathcal{P}(x,t)&=\mathcal{A}_2 e^{i(\alpha_1 x+\beta_1 t+\gamma_1)}\varphi(\alpha_2 x+\beta_2 t+\gamma_2)\end{aligned} \tag{3.2}$$

where x and t are real variables, α_j , β_j , γ_j ($j=1,2$) are real parameters, and $\mathcal{A}_1,\mathcal{A}_2$ are the maximum absolute values of the amplitudes. Moreover, a form of the single soliton solution for the discrete nonlocal NLS equation (DNNLS) (1.3) has been given in [2, 16, 24, 25, 30], and can also be described in the formula:

$$\mathcal{Q}_n(t)=\mathcal{A}e^{i(\alpha_1 n+\beta_1 t+\gamma_1)}\varphi(\alpha_2 n+\beta_2 t+\gamma_2) \tag{3.3}$$

where n is an integer variable while t is a real variable, whereas, $\mathcal{A}$, α_j , β_j , γ_j ($j = 1, 2$) are as in (3.1). Following from the formulas (3.1), (3.2) and (3.3), we select initial conditions for NDMS (1.4) in the form:

$$\begin{array}{l} \mathcal{Q}_n(0) = \mathcal{A}_1 e^{i(\alpha_1 n+\gamma_1)} \varphi(\alpha_2 n + \gamma_2) \\ \mathcal{P}_n(0) = \mathcal{A}_2 e^{i(\alpha_1 n+\gamma_1)} \varphi(\alpha_2 n + \gamma_2) \end{array} \tag{3.4}$$

where n is an integer variable, $\mathcal{A}_j$, α_j , γ_j ($j = 1, 2$) are the same as in (3.2), and φ is a function that describes the initial shape of the wave. Regarding periodic and solitary wave solutions, we consider three cases. The first case considers a constant function φ leading to periodic-wave solutions of constant amplitude. The second case considers φ as a hyperbolic secant related to the bright-soliton solution with a fast decaying boundary. The last case considers φ as a hyperbolic tangent leading to a dark-soliton solution with a non-zero constant boundary (see [7, 13, 40, 52, 53]).

Recall that the nonlocal discrete Manakov system NDMS considered here is written as:

$$\begin{array}{l} i\mathcal{Q}_{n,t} + (\mathcal{Q}_{n+1} - 2\mathcal{Q}_n + \mathcal{Q}_{n-1}) + \sigma\left(\mathcal{Q}_n\mathcal{Q}^*_{-n} + \mathcal{P}_n\mathcal{P}^*_{-n}\right)(\mathcal{Q}_{n+1} + \mathcal{Q}_{n-1}) = 0 \\ i\mathcal{P}_{n,t} + (\mathcal{P}_{n+1} - 2\mathcal{P}_n + \mathcal{P}_{n-1}) + \sigma(\mathcal{Q}_n\mathcal{Q}^*_{-n} + \mathcal{P}_n\mathcal{P}^*_{-n})(\mathcal{P}_{n+1} + \mathcal{P}_{n-1}) = 0 \end{array} \tag{3.5}$$

Here, $\mathcal{Q}^*_{-n}$, $\mathcal{P}^*_{-n}$ are the nonlocal complex conjugates of $\mathcal{Q}_n$, $\mathcal{P}_n$, respectively. According to an equation of the VIM, correction functionals for system (3.5) can be defined in the formula:

$$\begin{array}{l} \mathcal{Q}_{n,k+1}(t) = \mathcal{Q}_{n,k}(t) + \displaystyle\int_0^t \lambda_1(\tau) \left[\begin{array}{c} i\frac{d\mathcal{Q}_{n,k}(\tau)}{d\tau} + \left(\tilde{\mathcal{Q}}_{n+1,k}(\tau) - 2\tilde{\mathcal{Q}}_{n,k}(\tau) + \tilde{\mathcal{Q}}_{n-1,k}(\tau)\right) \\ +\sigma\left(\tilde{\mathcal{Q}}_{n,k}(\tau)\tilde{\mathcal{Q}}^*_{-n,k}(\tau) + \tilde{\mathcal{P}}_{n,k}(\tau)\tilde{\mathcal{P}}^*_{-n,k}(\tau)\right)\left(\tilde{\mathcal{Q}}_{n+1,k}(\tau) + \tilde{\mathcal{Q}}_{n-1,k}(\tau)\right) \end{array} \right] d\tau \\ \mathcal{P}_{n,k+1}(t) = \mathcal{P}_{n,k}(t) + \displaystyle\int_0^t \lambda_2(\tau) \left[\begin{array}{c} i\frac{d\mathcal{P}_{n,k}(\tau)}{d\tau} + \left(\tilde{\mathcal{P}}_{n+1,k}(\tau) - 2\tilde{\mathcal{P}}_{n,k}(\tau) + \tilde{\mathcal{P}}_{n-1,k}(\tau)\right) \\ +\sigma\left(\tilde{\mathcal{Q}}_{n,k}(\tau)\tilde{\mathcal{Q}}^*_{-n,k}(\tau) + \tilde{\mathcal{P}}_{n,k}(\tau)\tilde{\mathcal{P}}^*_{-n,k}(\tau)\right)\left(\tilde{\mathcal{P}}_{n+1,k}(\tau) + \tilde{\mathcal{P}}_{n-1,k}(\tau)\right) \end{array} \right] d\tau \end{array} \tag{3.6}$$

where, λ_1 and λ_2 represents the general Lagrange multipliers. The stationary conditions of the correction functionals in (3.6) are given by:

$$\begin{array}{ll} 1 + i\lambda_1(\tau)|_{\tau=t} = 0, & \dot{\lambda}_1(\tau)|_{\tau=t} = 0 \\ 1 + i\lambda_2(\tau)|_{\tau=t} = 0, & \dot{\lambda}_2(\tau)|_{\tau=t} = 0 \end{array} \tag{3.7}$$

Hence, the Lagrange multipliers can be obtained to be:

$$\begin{array}{l} \lambda_1(\tau) = i \\ \lambda_2(\tau) = i \end{array} \tag{3.8}$$

The iterative formula for $k \geq 0$ is induced by substituting (3.8) into (3.6) and getting:

$$\begin{array}{l} \mathcal{Q}_{n,k+1}(t) = \mathcal{Q}_{n,k}(t) + \displaystyle\int_0^t \lambda_1(\tau) \left[\begin{array}{c} i\frac{d\mathcal{Q}_{n,k}(\tau)}{d\tau} + (\mathcal{Q}_{n+1,k}(\tau) - 2\mathcal{Q}_{n,k}(\tau) + \mathcal{Q}_{n-1,k}(\tau)) \\ +\sigma\left(\mathcal{Q}_{n,k}(\tau)\mathcal{Q}^*_{-n,k}(\tau) + \mathcal{P}_{n,k}(\tau)\mathcal{P}^*_{-n,k}(\tau)\right)(\mathcal{Q}_{n+1,k}(\tau) + \mathcal{Q}_{n-1,k}(\tau)) \end{array} \right] d\tau \\ \mathcal{P}_{n,k+1}(t) = \mathcal{P}_{n,k}(t) + \displaystyle\int_0^t \lambda_2(\tau) \left[\begin{array}{c} i\frac{d\mathcal{P}_{n,k}(\tau)}{d\tau} + (\mathcal{P}_{n+1,k}(\tau) - 2\mathcal{P}_{n,k}(\tau) + \mathcal{P}_{n-1,k}(\tau)) \\ +\sigma\left(\mathcal{Q}_{n,k}(\tau)\mathcal{Q}^*_{-n,k}(\tau) + \mathcal{P}_{n,k}(\tau)\mathcal{P}^*_{-n,k}(\tau)\right)(\mathcal{P}_{n+1,k}(\tau) + \mathcal{P}_{n-1,k}(\tau)) \end{array} \right] d\tau \end{array} \tag{3.9}$$

Which will be used to construct the approximate solutions in section 5.

4 Error Measurement

This section is concerned with the least squares weighted function (LSWF) that will be used to measure the numerical simulation's error. Consider the non-homogeneous system:

$$\mathcal{D}z(x,t) = g(x,t) \tag{4.1}$$

where $\mathcal{D}$ denotes is a differential operator. Any exact solution $z(x,t)$ defined on a real interval $x \in I = [a,b]$ and $t \geq 0$ satisfies equation (4.1). Now, if we consider $\mathcal{Z}(x,t)$ as an approximate solution then equation (4.1) will not be completely satisfied. The residual error $\mathcal{R}(x,t)$ created by the approximation at a given point (x,t) in the domain can be given by:

$$\mathcal{R}(x,t) = \mathcal{D}\mathcal{Z}(x,t) - g(x,t) \tag{4.2}$$

The method of LSWF is used to calculate the total error induced by the residual of the approximate solution $\mathcal{Z}(x,t)$ over the domain, (see [1, 23, 44, 54]). Over the discretized time range $t = t_l$, ($l = 0, 1, \ldots, \mathcal{M}$), the LSWF can be computed for each integer n as follows:

$$\text{LSWF} = \frac{\sum_{l=0}^{\mathcal{M}} |\mathcal{R}(n,t_l)|^2}{\mathcal{M}+1} \tag{4.3}$$

The formula (4.3) will be used to measure and analyze the approximation error at each of the space lattice points.

5 Numerical Results

The approximate solution of the NDMS (3.5) obtained from the VIM is shown and discussed in this section. Bright-soliton and dark-soliton in addition to the periodic-wave have been considered in the following three subsections. MATLAB R2021a program was used to carry out the numerical computations and visualization.

5.1 Bright-Soliton Solutions

Here, we consider the focusing case $\sigma = +1$. To construct a bright-soliton solution of the NDMS, we select the initial conditions in equations (3.4) to be in the form:

$$\begin{aligned} \mathcal{Q}_n(0) &= \mathcal{A}_1 e^{i(\alpha_1 n+\gamma_1)} \operatorname{sech}(\alpha_2 n+\gamma_2) \\ \mathcal{P}_n(0) &= \mathcal{A}_2 e^{i(\alpha_1 n+\gamma_1)} \operatorname{sech}(\alpha_2 n+\gamma_2) \end{aligned} \tag{5.1}$$

where, $\mathcal{A}_1, \mathcal{A}_2$ are scalar constants, and α_j , γ_j ($j = 1, 2$) are real constants. Hence, the approximate solutions can be induced from the iterative formula (3.9) after substituting the initial condition (5.1) as follows:

$$\begin{aligned}
&\mathcal{Q}_{n,0}(t) = \mathcal{A}_1 e^{i(\alpha_1 n+\gamma_1)} \operatorname{sech}(\alpha_2 n+\gamma_2) \\
&\mathcal{P}_{n,0}(t) = \mathcal{A}_2 e^{i(\alpha_1 n+\gamma_1)} \operatorname{sech}(\alpha_2 n+\gamma_2) \\
&\mathcal{Q}_{n,1}(t) = \mathcal{A}_1 e^{i(\alpha_1 n+\gamma_1)} \operatorname{sech}(\alpha_2 n+\gamma_2) + \mathcal{A}_1 t i e^{i(\alpha_1+\alpha_1 n+\gamma_1)} \operatorname{sech}(\alpha_2+\alpha_2 n+\gamma_2) \\
&- 2\mathcal{A}_1 t i e^{i(\alpha_1 n+\gamma_1)} \operatorname{sech}(\alpha_2 n+\gamma_2) + \mathcal{A}_1 t i e^{i(-\alpha_1+\alpha_1 n+\gamma_1)} \operatorname{sech}(-\alpha_2+\alpha_2 n+\gamma_2) \\
&+ \sigma t i \left[\mathcal{A}_1^2 e^{2i\alpha_1 n} \operatorname{sech}(\alpha_2 n+\gamma_2) \operatorname{sech}(-\alpha_2 n+\gamma_2)\right. \\
&\left.+\mathcal{A}_2^2 e^{2i\alpha_1 n} \operatorname{sech}(\alpha_2 n+\gamma_2) \operatorname{sech}(-\alpha_2 n+\gamma_2)\right] \left[\mathcal{A}_1 e^{i(\alpha_1+\alpha_1 n+\gamma_1)} \operatorname{sech}(\alpha_2+\alpha_2 n+\gamma_2)\right. \\
&\left.+\mathcal{A}_1 e^{i(-\alpha_1+\alpha_1 n+\gamma_1)} \operatorname{sech}(-\alpha_2+\alpha_2 n+\gamma_2)\right] \\
&\mathcal{P}_{n,1}(t) = \mathcal{A}_2 e^{i(\alpha_1 n+\gamma_1)} \operatorname{sech}(\alpha_2 n+\gamma_2) + \mathcal{A}_2 t i e^{i(\alpha_1+\alpha_1 n+\gamma_1)} \operatorname{sech}(\alpha_2+\alpha_2 n+\gamma_2) \\
&- 2\mathcal{A}_2 t i e^{i(\alpha_1 n+\gamma_1)} \operatorname{sech}(\alpha_2 n+\gamma_2) + \mathcal{A}_2 t i e^{i(-\alpha_1+\alpha_1 n+\gamma_1)} \operatorname{sech}(-\alpha_2+\alpha_2 n+\gamma_2) \\
&+ \sigma t i \left[\mathcal{A}_1^2 e^{2i\alpha_1 n} \operatorname{sech}(\alpha_2 n+\gamma_2) \operatorname{sech}(-\alpha_2 n+\gamma_2)\right. \\
&\left.+\mathcal{A}_2^2 e^{2i\alpha_1 n} \operatorname{sech}(\alpha_2 n+\gamma_2) \operatorname{sech}(-\alpha_2 n+\gamma_2)\right] \left[\mathcal{A}_2 e^{i(\alpha_1+\alpha_1 n+\gamma_1)} \operatorname{sech}(\alpha_2+\alpha_2 n+\gamma_2)\right. \\
&\left.+\mathcal{A}_2 e^{i(-\alpha_1+\alpha_1 n+\gamma_1)} \operatorname{sech}(-\alpha_2+\alpha_2 n+\gamma_2)\right]
\end{aligned}$$

Following the same procedure, higher iterations can lead to the approximate solution of higher accuracy.

Table 1 shows the error of the numerical solution measured using the LSWF for selected constants' values. The estimated error in the table demonstrates that the approximated solution calculated from the third iteration of the

VIM is efficient in the time span $t \in [0, 1]$. The time evolution of the numerical bright-soliton wave solution is visualized in Figure 1 and Figure 2. A slight shift in the solitary wave peak can be noticed in Figure 2 as a result of the time progress.

Table 1: The absolute values of the approximate bright-soliton solution for the 3^{rd} iteration at $t = 1$ and the corresponding LSWF errors over $0 \leq t \leq 1$, calculated for different values of n with the constants' values $\mathcal{A}_1 = 0.3$, $\mathcal{A}_2 = -0.1$, $\alpha_1 = \alpha_2 = 0.5$, $\gamma_1 = \gamma_2 = 0$ and $\sigma = 1$.

n	$\lvert\mathcal{Q}_{n,3}(t)\rvert$	$\lvert\mathcal{P}_{n,3}(t)\rvert$	$E(\mathcal{Q}_{n,3}(t))$	$E(\mathcal{P}_{n,3}(t))$
-20	1.6464250e-05	5.4880834e-06	1.4501008e-14	1.6112230e-15
-15	2.0057554e-04	6.6858513e-05	2.1526301e-12	2.3918112e-13
-10	0.0024433	8.1441744e-04	3.4034045e-10	3.7815605e-11
-5	0.0292443	0.0097481	3.9776905e-06	4.4196560e-07
0	0.2719591	0.0906530	3.8372233e-05	4.2635816e-06
5	0.0818038	0.0272679	3.9626134e-06	4.4029036e-07
10	0.0066515	0.0022172	3.4033543e-10	3.7815046e-11
15	5.4599083e-04	1.8199695e-04	2.1526307e-12	2.3918118e-13
20	4.4817680e-05	1.4939227e-05	1.4501008e-14	1.6112230e-15

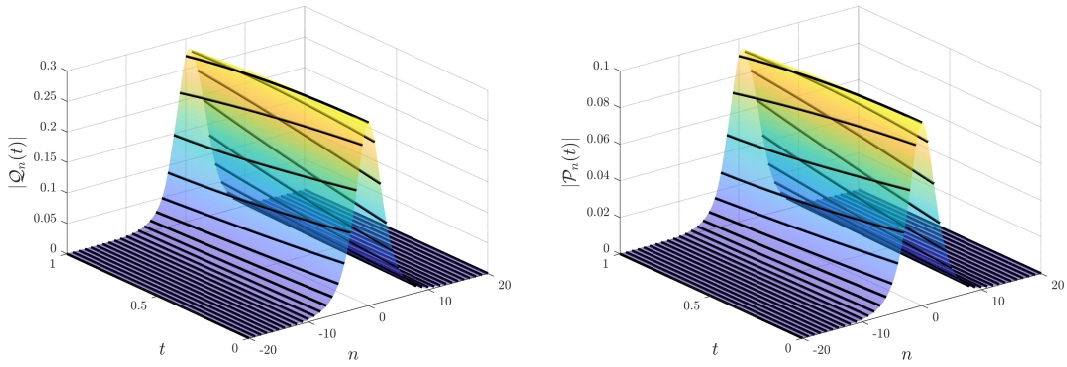

Figure 1: Absolute value of the approximate bright-soliton solution over the time period $0 \leq t \leq 1$ and discrete lattice $-20 \leq n \leq 20$, for the constants' values: $\mathcal{A}_1 = 0.3$, $\mathcal{A}_2 = -0.1$, $\alpha_1 = \alpha_2 = 0.5$, $\gamma_1 = \gamma_2 = 0$ and $\sigma = 1$.

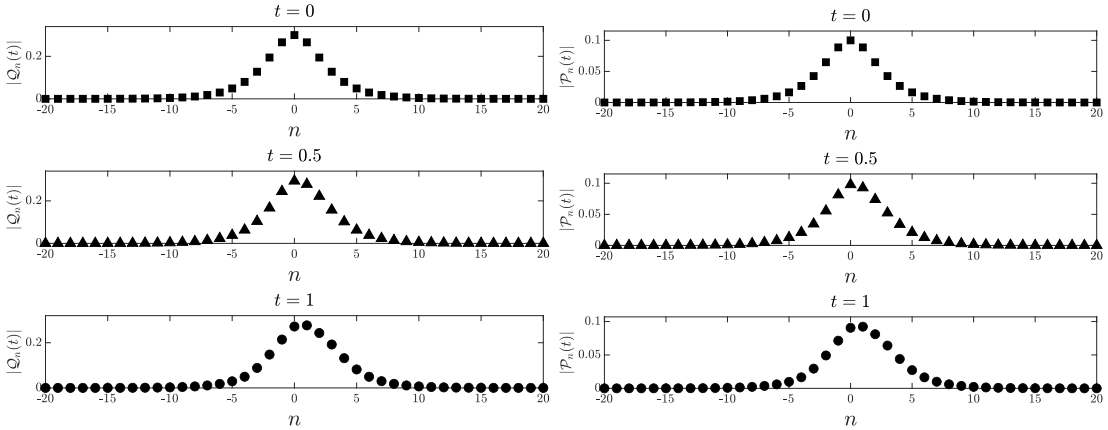

Figure 2: Time-shots of the absolute value for the approximate bright-soliton solution at $t = 0$, 0.5 and 1, over $-20 \leq n \leq 20$, with constants' values: $\mathcal{A}_1 = 0.3$, $\mathcal{A}_2 = -0.1$, $\alpha_1 = \alpha_2 = 0.5$, $\gamma_1 = \gamma_2 = 0$ and $\sigma = 1$.

5.2 Dark-Soliton Solutions

Consider now the defocusing case $\sigma = -1$. To construct a dark-soliton solution of the NDMS, we select the initial conditions in equations (3.4) to be in the form:

$$\begin{aligned} \mathcal{Q}_n(0) &= \mathcal{A}_1 e^{i(\alpha_1 n+\gamma_1)} \tanh(\alpha_2 n+\gamma_2) \\ \mathcal{P}_n(0) &= \mathcal{A}_2 e^{i(\alpha_1 n+\gamma_1)} \tanh(\alpha_2 n+\gamma_2) \end{aligned} \tag{5.2}$$

with the same constants' values of the case of bright-soliton solution. The approximate solutions can be induced from the iterative formula (3.9) after substituting the initial condition (5.2) as follows:

$$\begin{aligned}
&\mathcal{Q}_{n,0}(t) = \mathcal{A}_1 e^{i(\alpha_1 n+\gamma_1)} \tanh(\alpha_2 n+\gamma_2) \\
&\mathcal{P}_{n,0}(t) = \mathcal{A}_2 e^{i(\alpha_1 n+\gamma_1)} \tanh(\alpha_2 n+\gamma_2) \\
&\mathcal{Q}_{n,1}(t) = \mathcal{A}_1 e^{i(\alpha_1 n+\gamma_1)} \tanh(\alpha_2 n+\gamma_2) + \mathcal{A}_1 t i e^{i(\alpha_1+\alpha_1 n+\gamma_1)} \tanh(\alpha_2+\alpha_2 n+\gamma_2) \\
&- 2\mathcal{A}_1 t i e^{i(\alpha_1 n+\gamma_1)} \tanh(\alpha_2 n+\gamma_2) + \mathcal{A}_1 t i e^{i(-\alpha_1+\alpha_1 n+\gamma_1)} \tanh(-\alpha_2+\alpha_2 n+\gamma_2) \\
&+ \sigma t i \left[\mathcal{A}_1^2 e^{2i\alpha_1 n} \tanh(\alpha_2 n+\gamma_2) \tanh(-\alpha_2 n+\gamma_2)\right. \\
&\left.+\mathcal{A}_2^2 e^{2i\alpha_1 n} \tanh(\alpha_2 n+\gamma_2) \tanh(-\alpha_2 n+\gamma_2)\right] \Big[\mathcal{A}_1 e^{i(\alpha_1+\alpha_1 n+\gamma_1)} \tanh(\alpha_2+\alpha_2 n+\gamma_2) \\
&+\mathcal{A}_1 e^{i(-\alpha_1+\alpha_1 n+\gamma_1)} \tanh(-\alpha_2+\alpha_2 n+\gamma_2)\Big] \\
&\mathcal{P}_{n,1}(t) = \mathcal{A}_2 e^{i(\alpha_1 n+\gamma_1)} \tanh(\alpha_2 n+\gamma_2) + \mathcal{A}_2 t i e^{i(\alpha_1+\alpha_1 n+\gamma_1)} \tanh(\alpha_2+\alpha_2 n+\gamma_2) \\
&- 2\mathcal{A}_2 t i e^{i(\alpha_1 n+\gamma_1)} \tanh(\alpha_2 n+\gamma_2) + \mathcal{A}_2 t i e^{i(-\alpha_1+\alpha_1 n+\gamma_1)} \tanh(-\alpha_2+\alpha_2 n+\gamma_2) \\
&+ \sigma t i \left[\mathcal{A}_1^2 e^{2i\alpha_1 n} \tanh(\alpha_2 n+\gamma_2) \tanh(-\alpha_2 n+\gamma_2)\right. \\
&\left.+\mathcal{A}_2^2 e^{2i\alpha_1 n} \tanh(\alpha_2 n+\gamma_2) \tanh(-\alpha_2 n+\gamma_2)\right] \Big[\mathcal{A}_2 e^{i(\alpha_1+\alpha_1 n+\gamma_1)} \tanh(\alpha_2+\alpha_2 n+\gamma_2) \\
&+\mathcal{A}_2 e^{i(-\alpha_1+\alpha_1 n+\gamma_1)} \tanh(-\alpha_2+\alpha_2 n+\gamma_2)\Big]
\end{aligned}$$

Following the same procedure, higher iterations can lead to the approximate solution of higher accuracy.

Table 2 shows the error of the numerical solution measured using the LSWF for selected constants' values. The estimated error in the table demonstrates that the approximated solution calculated from the third iteration of the VIM is efficient in the time span $t \in [0, 1]$. The time evolution of the numerical dark-soliton wave solution is visualized in Figure 3 and Figure 4. A slight shift in the solitary wave bottom can be noticed in Figure 4 as a result of the time progress.

Table 2: The absolute values of the approximate dark-soliton solution for the 3^{rd} iteration at $t = 1$ and the corresponding LSWF errors over $0 \le t \le 1$, calculated for different values of n with the constants' values $\mathcal{A}_1 = 0.3$, $\mathcal{A}_2 = -0.1$, $\alpha_1 = \alpha_2 = 0.4$, $\gamma_1 = \gamma_2 = 0$ and $\sigma = -1$.

n	$\lvert\mathcal{Q}_{n,3}(t)\rvert$	$\lvert\mathcal{P}_{n,3}(t)\rvert$	$E(\mathcal{Q}_{n,3}(t))$	$E(\mathcal{P}_{n,3}(t))$
-20	0.2741852	0.0913951	7.5769094e-05	8.4187886e-06
-15	0.3018085	0.1006028	1.1530594e-05	1.2811771e-06
-10	0.3244254	0.1081418	4.8131533e-05	5.3479484e-06
-5	0.2654129	0.0884710	7.4597236e-05	8.2885808e-06
0	0.0823215	0.0274405	1.4968765e-04	1.6631961e-05
5	0.2851589	0.0950530	7.3969386e-05	8.2188208e-06
10	0.2729720	0.0909907	4.9776285e-05	5.5306987e-06
15	0.3328356	0.1109452	1.0034170e-05	1.1149077e-06
20	0.2880382	0.0960127	7.5137206e-05	8.3485784e-06

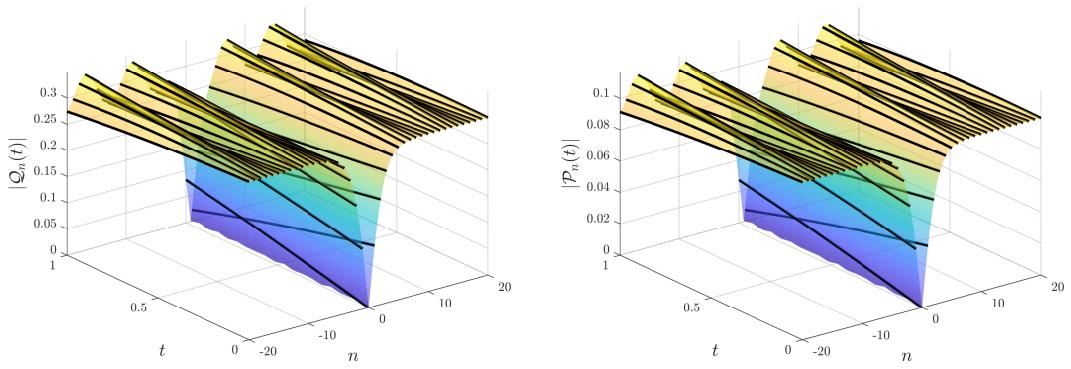

Figure 3: Absolute value of the approximate dark-soliton solution over the time period $0 \leq t \leq 1$ and discrete lattice $-20 \leq n \leq 20$, for the constants' values: $\mathcal{A}_1 = 0.3,\ \mathcal{A}_2 = -0.1,\ \alpha_1 = \alpha_2 = 0.4,\ \gamma_1 = \gamma_2 = 0$ and $\sigma = -1$.

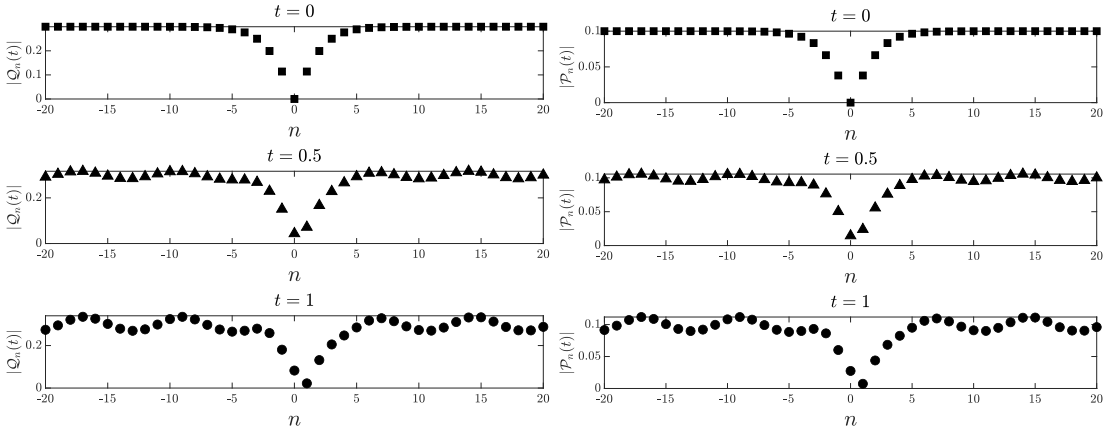

Figure 4: Time-shots of the absolute value for the approximate dark-soliton solution at $t = 0,\ 0.5$ and 1, over $-20 \leq n \leq 20$, with constants' values: $\mathcal{A}_1 = 0.3,\ \mathcal{A}_2 = -0.1,\ \alpha_1 = \alpha_2 = 0.4,\ \gamma_1 = \gamma_2 = 0$ and $\sigma = -1$.

5.3 Periodic-Wave Solutions

Considering focusing case $\sigma = +1$, we can construct a periodic-wave solution of the NDMS by selecting initial conditions with constant amplitude as follows:

$$\begin{aligned} \mathcal{Q}_n(0) &= \mathcal{A}_1 e^{i(\alpha_1 n + \gamma_1)} \\ \mathcal{P}_n(0) &= \mathcal{A}_2 e^{i(\alpha_1 n + \gamma_1)} \end{aligned} \tag{5.3}$$

where, $\mathcal{A}_1, \mathcal{A}_2$ are scalar constants, while a_1 , γ_1 are real constants. Then, the approximate solutions can be induced from the iterative formula (3.9) after substituting the initial condition (5.3) as follows:

$$\begin{aligned} &\mathcal{Q}_{n,0}(t) = \mathcal{A}_1 e^{i(\alpha_1 n + \gamma_1)} \\ &\mathcal{P}_{n,0}(t) = \mathcal{A}_2 e^{i(\alpha_1 n + \gamma_1)} \\ &\mathcal{Q}_{n,1}(t) = \mathcal{A}_1 e^{i(\alpha_1 n + \gamma_1)} + \mathcal{A}_1 t i e^{i(\alpha_1 + \alpha_1 n + \gamma_1)} - 2\mathcal{A}_1 t i e^{i(\alpha_1 n + \gamma_1)} + \mathcal{A}_1 t i e^{i(-\alpha_1 + \alpha_1 n + \gamma_1)} \\ &+ \sigma t i \left[\mathcal{A}_1^2 e^{2i\alpha_1 n} + \mathcal{A}_2^2 e^{2i\alpha_1 n}\right] \left[\mathcal{A}_1 e^{i(\alpha_1 + \alpha_1 n + \gamma_1)} + \mathcal{A}_1 e^{i(-\alpha_1 + \alpha_1 n + \gamma_1)}\right] \\ &\mathcal{P}_{n,1}(t) = \mathcal{A}_2 e^{i(\alpha_1 n + \gamma_1)} + \mathcal{A}_2 t i e^{i(\alpha_1 + \alpha_1 n + \gamma_1)} - 2\mathcal{A}_2 t i e^{i(\alpha_1 n + \gamma_1)} + \mathcal{A}_2 t i e^{i(-\alpha_1 + \alpha_1 n + \gamma_1)} \\ &+ \sigma t i \left[\mathcal{A}_1^2 e^{2i\alpha_1 n} + \mathcal{A}_2^2 e^{2i\alpha_1 n}\right] \left[\mathcal{A}_2 e^{i(\alpha_1 + \alpha_1 n + \gamma_1)} + \mathcal{A}_2 e^{i(-\alpha_1 + \alpha_1 n + \gamma_1)}\right] \end{aligned}$$

Following the same procedure, higher iterations can lead to the approximate solution of higher accuracy.

Table 3. shows the error of the numerical solution measured using the LSWF for selected constants' values. The estimated error in the table demonstrates that the approximated solution is efficient in the time span $t \in [0, 1]$. The time evolution of the numerical periodic wave solution is visualized in Figure 5 and Figure 6.

Table 3: The real part (Re) of the approximate periodic-wave solution for the 3^{rd} iteration at $t = 1$ and the corresponding LSWF errors over $0 \leq t \leq 1$, calculated for different values of n with the constants' values $\mathcal{A}_1 = 0.4,\ \mathcal{A}_2 = -0.3,\ \alpha_1 = 0.5\ ,\ \gamma_1 = 0$ and $\sigma = 1$.

n	$\mathbf{Re}\,(\mathcal{Q}_{n,3}(t))$	$\mathbf{Re}\,(\mathcal{P}_{n,3}(t))$	$E\,(\mathbf{Re}\,(\mathcal{Q}_{n,3}(t)))$	$E\,(\mathbf{Re}\,(\mathcal{P}_{n,3}(t)))$
-20	-0.2780198	0.2085149	1.9004996e-04	1.0690309e-04
-15	0.0128483	-0.0096362	1.7896421e-04	1.0066738e-04
-10	0.1865238	-0.1398929	7.4048927e-05	4.1652525e-05
-5	-0.3499268	0.2624451	1.9099512e-04	1.0743476e-04
0	0.4174657	-0.3130993	1.4841213e-04	8.3481827e-05
5	-0.2514621	0.1885965	1.8245350e-04	1.0263010e-04
10	-0.0114263	0.0085698	8.1624596e-05	4.5913832e-05
15	0.2044084	-0.1533063	1.7648627e-04	9.9273522e-05
20	-0.3641605	0.2731203	1.9852690e-04	1.1167138e-04

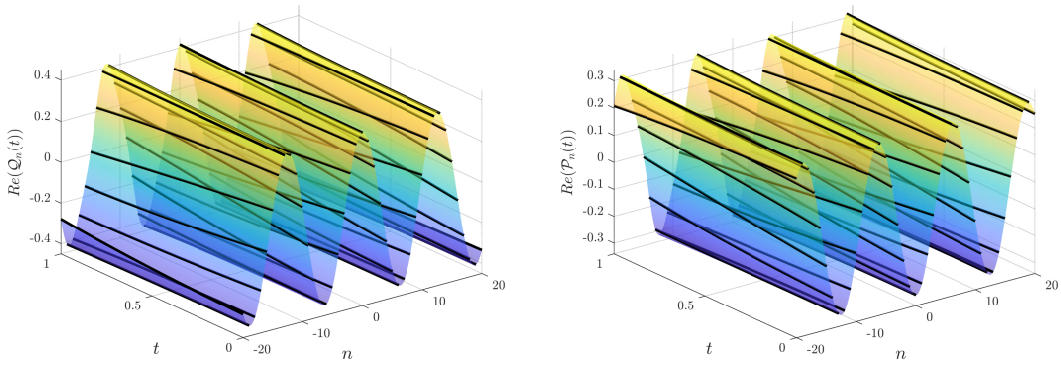

Figure 5: The real part of the approximate periodic-wave solution over the time period $0 \leq t \leq 1$ and discrete lattice $-20 \leq n \leq 20$, for the constants' values: $\mathcal{A}_1 = 0.4,\ \mathcal{A}_2 = -0.3,\ \alpha_1 = 0.5,\ \gamma_1 = 0$ and $\sigma = 1$.

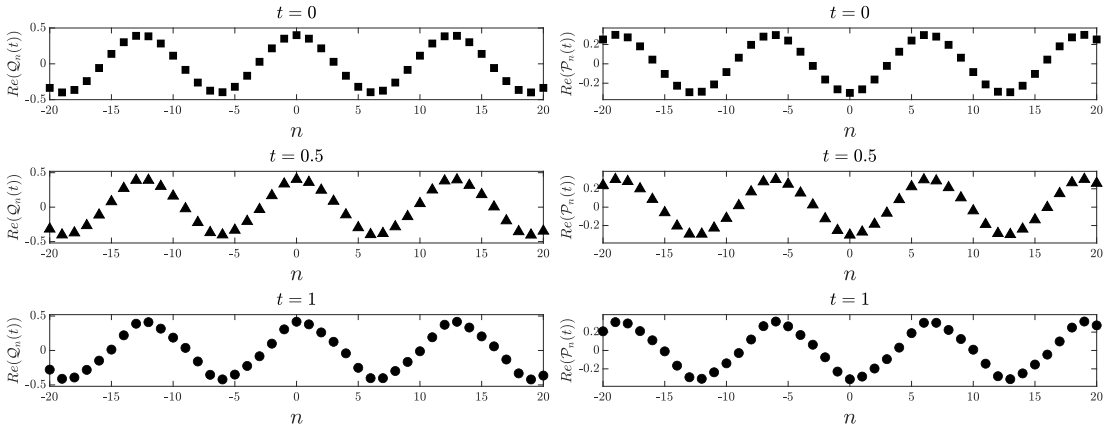

Figure 6: Time-shots of the real part for the approximate periodic-wave solution at $t = 0,\ 0.5$ and 1, over $-20 \leq n \leq 20$, with constants' values: $\mathcal{A}_1 = 0.4,\ \mathcal{A}_2 = -0.3,\ \alpha_1 = 0.5\ ,\ \gamma_1 = 0$ and $\sigma = 1$.

6 Conclusion

In this work, a discrete version of the nonlocal Manakov system has been proposed and shown to satisfy the PT-symmetry property which requires the invariance of the system under reversing time and position variables after taking the complex conjugate. Three types of wave solutions have been simulated for the system using the variational iteration method (VIM). By choosing appropriate initial conditions, the system shows to support bright and dark solitons in addition to the periodic waves. The solitary waves translate over the space lattice as time progresses. The error measurement of the simulation demonstrates the efficiency of the numerically computed time evolution of the system in the explored range of time. Extending the time span can lead to increasing the simulation error due to the fact that the approximated solutions constructed from the VIM are polynomials in the time variable. These polynomials are unbounded with time; therefore, higher iteration is required to induce a good approximation of the system solutions via the VIM technique.

References

[1] A.T. Abed and A.S.Y. Aladool, *Applying particle swarm optimization based on Padé approximant to solve ordinary differential equation*, Numer. Algebr. Control Optim. **12** (2022), 321—337.

[2] M.J. Ablowitz, X.D. Luo and Z.H. Musslimani, *Discrete nonlocal nonlinear Schrödinger systems: Integrability, inverse scattering and solitons*, Nonlinearity **33** (2020), 3653—3707.

[3] M.J. Ablowitz and Z.H. Musslimani, *Integrable nonlocal nonlinear Schrödinger equation*, Phys. Rev. Lett. **110** (2013), 64105.

[4] M.J. Ablowitz and Z.H. Musslimani, *Integrable discrete PT symmetric model*, Phys. Rev. E - Stat. Nonlinear, Soft Matter Phys. **90** (2014), 32912.

[5] M. J. Ablowitz and Musslimani, Z. H. Musslimani, *Integrable nonlocal nonlinear equations*, Stud. Appl. Math. **139** (2017), 7-–59.

[6] M. Akbarzade and J. Langari, *Application of variational iteration method to partial differential equation systems*, Int. J. Math. Anal. **5** (2011), 863-–870.

[7] T. Aktosun, F. Demontis and C.V.D. Mee, *Exact solutions to the focusing nonlinear Schrödinger equation*, Inverse Probl. **23** (2007), 2171—2195.

[8] C.M. Bender, *Introduction to PT-symmetric quantum theory*, Contemp. Phys. **46** (2005), 277—292.

[9] C.M. Bender, *Making sense of non-Hermitian Hamiltonians*, Reports Prog. Phys. **70** (2007), 947.

[10] C.M. Bender and S. Boettcher, *Real spectra in non-hermitian hamiltonians having PT symmetry*, Phys. Rev. Lett. **80** (1998), 5243-–5246.

[11] A. Beygi, S.P. Klevansky and C.M. Bender, *Coupled oscillator systems having partial PT symmetry*, Phys. Rev. A - At. Mol. Opt. Phys. **91** (2015), 62101.

[12] N. Bildik and A. Konuralp, *The use of variational iteration method, differential transform method and adomian decomposition method for solving different types of nonlinear partial differential equations*, Int. J. Nonlinear Sci. Numer. Simul. **7** (2006), 65—70.

[13] A. Bratsos, M. Ehrhardt and I.T. Famelis, *A discrete Adomian decomposition method for discrete nonlinear Schrödinger equations*, Appl. Math. Comput. **197** (2008), 190—205.

[14] R. El-Ganainy, K. G. Makris, M. Khajavikhan, Z. H. Musslimani, S. Rotter and D.N. Christodoulides, *Non-Hermitian physics and PT symmetry*, Nat. Phys. **14** (2017), 11-–19.

[15] T.A. Gadzhimuradov and A.M. Agalarov, *Towards a gauge-equivalent magnetic structure of the nonlocal nonlinear Schrödinger equation*, Phys. Rev. A **93** (2016), 62124.

[16] G.G. Grahovski, A.J. Mohammed and H. Susanto, *Nonlocal Reductions of the Ablowitz–Ladik Equation*, Theor. Math. Phys. Russian Fed. **197** (2018), 1412—1429.

[17] G.G. Grahovski, J.I. Mustafa and H. Susanto, *Nonlocal reductions of the multicomponent nonlinear Schrödinger equation on symmetric spaces*, Theor. Math. Phys. **197** (2018), 1430—1450.

[18] A. Guo and G.J. Salamo, *Observation of PT-symmetry breaking in complex optical potentials*, Phys. Rev. Lett. **103** (2009), 93902.

[19] J.H. He, *Variational iteration method - A kind of non-linear analytical technique: Some examples*, Int. J. Nonlnear. Mech. **34** (1999), 699—708.

[20] X. Huang and L. Ling, *Soliton solutions for the nonlocal nonlinear Schrödinger equation*, Eur. Phys. J. Plus **131** (2016), 1—11.

[21] J.L. Ji, Z.W. Xu and Z.N. Zhu, *Nonintegrable spatial discrete nonlocal nonlinear schrödinger equation*, Chaos **29** (2019), 103129.

[22] Y.V. Kartashov, V.V. Konotop and L. Torner, *Topological States in Partially-$\mathcal{PT}$-Symmetric Azimuthal Potentials*, Phys. Rev. Lett. **115** (2015), 193902.

[23] K.B. Kazemi, *Solving differential equations with least square and collocation methods*, UNLV Theses, Diss. Prof. Pap. Capstones **66** (2015).

[24] A. Khare and A. Saxena, *Periodic and hyperbolic soliton solutions of a number of nonlocal nonlinear equations*, J. Math. Phys. **56** (2015), 32104.

[25] A. Khare, A. Saxena and A. Khare, *Solutions of several coupled discrete models in terms of Lamé polynomials of arbitrary order*, Pramana J. Phys. **79** (2012), 377-–392.

[26] V.V. Konotop, J. Yang and D.A. Zezyulin, *Nonlinear waves in $\mathcal{PT}$-symmetric systems*, Rev. Mod. Phys. **88** (2016), 35002.

[27] T. Kottos, *Broken symmetry makes light work*, Nat. Phys. **6** (2010), 166-–167.

[28] J. Liu, *Reductions of nonlocal nonlinear Schrödinger equations to Painlev'e type functions*, arXiv Prepr. arXiv2104, (2021), 10589.

[29] Y.C. Liu and C.S. Gurram, *Solving nonlinear differential difference equations using He's variational iteration method*, Appl. Math. Comput. Sci. **3** (2011).

[30] L.Y. Ma and Z.N. Zhu, *N-soliton solution for an integrable nonlocal discrete focusing nonlinear Schrödinger equation*, Appl. Math. Lett. **59** (2016), 115–121.

[31] L.Y. Ma and Z.N. Zhu, *Nonlocal nonlinear Schrödinger equation and its discrete version: Soliton solutions and gauge equivalence*, J. Math. Phys. **57** (2016), 83507.

[32] K.G. Makris, R. El-Ganainy, D.N. Christodoulides and Z.H. Musslimani, *Beam dynamics in PT symmetric optical lattices*, Phys. Rev. Lett. **100** (2008), 103904.

[33] S.V. Manakov, *On the theory of two-dimensional stationary self-focusing of electromagnetic waves*, Sov. Physics-JETP **38** (1974), 248-–253.

[34] H.K. Mishra, *A Comparative Study of Variational Iteration Method and He-Laplace Method*, Appl. Math. **03** (2012), 1193—1201.

[35] M. Mitchell, M. Segev, T.H. Coskun and D.N. Christodoulides, *Theory of self-trapped spatially incoherent light beams*, Phys. Rev. Lett. **79** (1997), 4990.

[36] S.T. Mohyud-Din and M.A. Noor, *Variational iteration method for solving discrete KdV equation*, Bull. Inst. Acad. Sin. **5** (2010), no. 1, 69–73.

[37] Z.H. Musslimani, K.G. Makris, R. El-Ganainy and D.N. Christodoulides, *Optical solitons in PT periodic potentials*, Conf. Quantum Electron. Laser Sci. Tech. Dig. Ser. **100** (2008), 30402.

[38] N. Okiotor, F. Ogunfiditimi and M.O. Durojaye, *On the computation of the Lagrange multiplier for the variational iteration ,ethod (VIM) for solving differential equations*, J. Adv. Math. Comput. Sci. **35** (2020), no. 3, 74-–92.

[39] J. Patra, *Some problems on variational iteration method*, MSc thesis, Department of Mathematics, National Institute of Technology Rourkela-769008, 2015.

[40] D.E. Pelinovsky and V.M. Rothos, *Bifurcations of travelling wave solutions in the discrete NLS equations*, Phys. D Nonlinear Phenom. **202** (2005), 16-–36.

[41] A. Regensburger, C. Bersch, M.A. Miri, G. Onishchukov, D.N. Christodoulides and U. Peschel, *Parity-time synthetic photonic lattices*, Nature **488** (2012), 167–171.

[42] A. Ruschhaupt, F. Delgado and J.G. Muga, *Physical realization of PT-symmetric potential scattering in a planar slab waveguide*, J. Phys. A. Math. Gen. **38** (2005), L171.

[43] C.E. Rüter, K.G. Makris, R. El-Ganainy, D.N. Christodoulides, M. Segev and D. Kip, *Observation of parity-time symmetry in optics*, Nat. Phys. **6** (2010), 192-–195.

[44] A. Sadollah, H. Eskandar, D.G. Yoo and J.H. Kim, *Approximate solving of nonlinear ordinary differential equations using least square weight function and metaheuristic algorithms*, Eng. Appl. Artif. Intell. **40** (2015), 117—132.

[45] D. Sinha and P.K. Ghosh, *Integrable nonlocal vector nonlinear Schrödinger equation with self-induced parity-time-symmetric potential*, Phys. Lett. Sect. A Gen. At. Solid State Phys. **381** (2017), 124-–128.

[46] S. Stalin, M. Senthilvelan and M. Lakshmanan, *Degenerate soliton solutions and their dynamics in the nonlocal Manakov system: II Interactions between solitons*, arXiv Prepr. arXiv1806. (2018), 06735.

[47] S. Stalin, M. Senthilvelan and M. Lakshmanan, *Degenerate soliton solutions and their dynamics in the nonlocal Manakov system: I symmetry preserving and symmetry breaking solutions*, Nonlinear Dyn. **95** (2019), 343—360.

[48] S.V. Suchkov, A.A. Sukhorukov, J. Huang, S.V. Dmitriev, C. Lee and Y.S. Kivshar, *Nonlinear switching and solitons in PT-symmetric photonic systems*, Laser Photonics Rev. **10** (2016), 177-–213.

[49] B. Sun, *General soliton solutions to a nonlocal long-wave–short-wave resonance interaction equation with nonzero boundary condition*, Nonlinear Dyn. **92** (2018), 1369—1377.

[50] N.H. Sweilam, *Variational iteration method for solving cubic nonlinear Schrödinger equation*, J. Comput. Appl. Math. **207** (2007), 155-–163.

[51] A.M. Wazwaz, *Partial Differential Equations and Solitary Waves Theory*, Higher Education Press, 2009.

[52] A.M. Wazwaz, *A variety of optical solitons for nonlinear Schrödinger equation with detuning term by the variational iteration method*, Optik (Stuttg) **196** (2019), 163169.

[53] A.M. Wazwaz, *Optical bright and dark soliton solutions for coupled nonlinear Schrödinger (CNLS) equations by the variational iteration method*, Optik (Stuttg) **207** (2020), 164457.

[54] J. Wu, *Least squares methods for solving partial differential equations by using Bézier control points*, Appl. Math. Comput. **219** (2012), 3655-–3663.

[55] J. Yang, *Physically significant nonlocal nonlinear Schrödinger equation and its soliton solutions*, Phys. Rev. E **98** (2018), 42202.

[56] B. Yang and Y. Chen, *General rogue waves and their dynamics in several reverse time integrable nonlocal nonlinear equations*, arXiv Prepr. arXiv1712, (2017), 05974.

[57] A. Yildirim, *Applying He's variational iteration method for solving differential-difference equation*, Math. Probl. Eng. **2008** (2008).

[58] G. Zhang and Z. Yan, *Multi-rational and semi-rational solitons and interactions for the nonlocal coupled nonlinear Schrödinger equations*, Epl **118** (2017), 60004.

[59] Y. Zhang, Y. Liu and X. Tang, *A general integrable three-component coupled nonlocal nonlinear Schrödinger equation*, Nonlinear Dyn. **89** (2017), 2729-–2738.

[60] H.Q. Zhang, M.Y. Zhang and R. Hu, *Darboux transformation and soliton solutions in the parity-time-symmetric nonlocal vector nonlinear Schrödinger equation*, Appl. Math. Lett. **76** (2018), 170-–174.